



Towards standardisation of surface electromyography measurements in the horse: Bipolar electrode location

I.H. Smit^{a,*}, J.I.M. Parmentier^{a,b}, T. Rovel^a, J. van Dieën^c, F.M. Serra Bragança^{a,d}

^a Department of Clinical Sciences, Faculty of Veterinary Medicine, Utrecht University, 3584CM Utrecht, the Netherlands

^b Pervasive Systems Group, Faculty of Electrical Engineering, Mathematics and Computer Science, University of Twente, 7522NB Enschede, the Netherlands

^c Department of Human Movement Sciences, Vrije Universiteit Amsterdam, Amsterdam Movement Sciences, Amsterdam, Netherlands

^d Sleip AI, Birger Jarlgatan 58, 11426 Stockholm, Sweden

ARTICLE INFO

Keywords:

Equine
sEMG
Methodology
Gait
Electrode array

ABSTRACT

The use of surface electromyography in the field of animal locomotion has increased considerably over the past decade. However, no consensus exists on the methodology for data collection in horses. This study aimed to start the development of recommendations for bipolar electrode locations to collect surface electromyographic data from horses during dynamic tasks.

Data were collected from 21 superficial muscles of three horses during trot on a treadmill using linear electrode arrays. The data were assessed both quantitatively (signal-to-noise ratio (SNR) and coefficient of variation (CoV)) and qualitatively (presence of crosstalk and activation patterns) to compare and select electrode locations for each muscle.

For most muscles and horses, the highest SNR values were detected near or cranial/proximal to the central region of the muscle. Concerning the CoV, there were larger differences between muscles and horses than within muscles. Qualitatively, crosstalk was suspected to be present in the signals of twelve muscles but not in all locations in the arrays.

With this study, a first attempt is made to develop recommendations for bipolar electrode locations for muscle activity measurements during dynamic contractions in horses. The results may help to improve the reliability and reproducibility of study results in equine biomechanics.

1. Introduction

Surface electromyography (EMG), a non-invasive technique to assess muscle activity, has received an increasing interest in equine locomotion research (Valentin and Zsoldos, 2017). This aligns with the increased popularity of gait analysis used in equine biomechanics to detect and quantify lameness (i.e., pain during locomotion) (Bragança et al., 2018). In addition, several technical advances, mainly wireless measurement options, have enabled the use of this technique to evaluate animals during natural tasks. This can provide valuable insights into the neuromuscular system in both healthy and pathological conditions and allow for a better understanding of the complex biomechanics of animal locomotion.

Despite the technical advances in surface EMG, divergence in methodology between research groups has limited the comparability and repeatability of study results. In an attempt to standardise the

methodology used to study muscle activity in humans, the SENIAM (Surface Electromyography for the Non-Invasive Assessment of Muscles) project (Hermens et al., 2000), the International Society of Electromyography and Kinesiology (ISEK) guidelines (Merletti, 1999) and more recently, the Consensus for Experimental Design in Electromyography (CEDE) project (Besomi et al., 2020, 2019) have been established. These projects provide considerations for bipolar (SENIAM) and multichannel (CEDE) data collection, signal processing (CEDE) and how to report the results (CEDE, ISEK guidelines), improving the repeatability and reliability of human studies. This has resulted in a large, more reliable body of evidence on human locomotion.

Obtaining a representative and robust estimation of muscle activity is essential in fundamental veterinary research, rehabilitation and sports applications. In human muscles, though not expected to be different from equine muscles, the detected signal is known to be affected by the detection system (e.g. electrode size and position (De Luca, 1997; Farina

* Corresponding author.

E-mail address: i.h.smit@uu.nl (I.H. Smit).

<https://doi.org/10.1016/j.jelekin.2024.102884>

Received 20 September 2023; Received in revised form 15 March 2024; Accepted 30 March 2024

Available online 1 April 2024

1050-6411/© 2024 The Authors. Published by Elsevier Ltd. This is an open access article under the CC BY-NC license (<http://creativecommons.org/licenses/by-nc/4.0/>).

et al., 2002; Hermens et al., 2000; Sacco et al., 2009)), by the type of contraction (either dynamic or static) (De Luca, 1997; Komi et al., 2000; Madeleine et al., 2001; Nakazawa et al., 1993) and other factors affecting the recording of surface EMGs in general, such as muscle architecture, skin preparation and adipose tissue (De Luca, 1997; Farina et al., 2002). Using surface EMG in horses, or animals in general, poses additional challenges compared to using this technique in humans. Examples of such challenges were outlined by Valentin and Zsoldos, which

include but are not limited to: (1) how to prepare densely hairy and greasy skin in order to ensure electrode adhesion and to minimise skin impedance; (2) behavioural constraints, such as the impossibilities or difficulties to acquire a maximal voluntary contraction for normalisation purposes, to repeat specific movements, or to perform isometric contractions; and (3) electrode positioning on the muscles of interest, specifically in animals with large muscles such as the horse (Valentin and Zsoldos, 2017). Among these, the position of the detection electrodes

Table 1

Anatomical landmarks used for electrode placement. Safe zones are presented as the percentage (%) between anatomical landmarks measured from the proximal or cranial landmark. For the m. rectus abdominis and m. pectoralis pars descendens the distance is given in centimeters (cm). All channels for the m. deltoideus were excluded, therefore no safe zones are indicated for this muscle.

Muscle	Proximal/Cranial	Distal/Caudal	Additional information	Safe zone per horse			Common safe zone
				Horse 1	Horse 2	Horse 3	
Biceps femoris	caudal part of the greater trochanter of the femur	lateral tibial condyle and head of the fibula		24–50 %	19–45.5 %	15.5–37 %	24–37 %
Brachiocephalicus	wing of the atlas	caudal part of the greater tuberosity of the humerus		47.5–60 %	32.5–42.5 % 50–57.5 %	41–64.5 %	50–57.5 %
Deltoideus	tip of the spina scapula	lateral side of the caput radii/ tuberositas radialis					
Extensor digitorum communis	lateral tuberosity of the radius	lateral styloid process of the radius - ventral side		27–50 %	30–47 %	12–43.5 %	30–43.5 %
Extensor carpi radialis	lacerus fibrosus	medial styloid process of the radius		28.5–47 %	53–72 %	39–50 %	none
Extensor digitorum lateralis	lateral tibial condyle and head of the fibula	lateral ridge of trochlea of talus		22–50 %	26–53.5 %	20–32 %	26–32 %
Extensor digitorum longus	tibial tuberosity	lateral ridge of trochlea of talus		30% – 50 %	42–53 %	36–71 %	42–50 %
Flexor carpi ulnaris	lateral tuberosity of the radius	accessory carpal bone		31.5–42 %	42.5–52.5 %	39–55.5 %	39–42 %
Flexor digitorum profundus	lateral tibial condyle and head of the fibula	calcaneal tubor		43.5–63 %	26.5–53.5 %	62.5–68.5 %	none
Gluteus medius	processus spinosus of L4	tuber ischiadicum			17.5–35 % 50 % 56 % 41–48 %	32–50 %	32–35 %
Latissimus dorsi	processus spinosus L4	cranial part of the greater tuberosity of the humerus	only one horse				
Longissimus	start of mane/top of the withers	between the tuber sacrale	6 cm out of the midline of the horse (processus spinosus)	40.5–57 %	41.5–61.5 %	45–62 %	45–57 %
Pectoralis descendens	manubrium of the sternum	Lacertus fibrosus		18–39.5 %	39–58 %	34.5–65 %	39–39.5 %
Petoralis ascendens	olecranon	no caudal landmark	3 finger widths out of the midline of the horse. Distance indicated in cm from cranial landmark.	2.4–4.8 cm 9.6–12.0 cm	2.4–7.2 cm	caudal of the olecranon	2.4–4.8 cm caudal of the olecranon
Rectus abdominis	no cranial landmark	Umbilicus	3 finger widths out of the midline of the horse. Distance indicated in cm from caudal landmark.	2.4–19.2 cm cranial from the umbilicus	2.4–19.2 cm cranial from the umbilicus	2.4 cm –16.8 cm cranial from the umbilicus	2.4–16.8 cm cranial from the umbilicus
Semitendinosus	tuber ischiadicum	at the height of the insertion of the gracilis		27.5–50 %	26–56 %	44–68 %	27.5–50 %
Splenius	wing of the atlas	cranial angle of the scapula		31–40.5 % 56.5–62.5 %	51.5–61.5 %	34–59.5 %	56.5–59.5 %
Triceps brachii, caput laterale	cranial part of the greater tuberosity of the humerus	olecranon		50–67.5 %	56–68 %	38–68 %	56–67.5 %
Triceps brachii, caput longum	tip of the spina scapula	olecranon		36–53.5 %	43–64.5 %	43.5–53.5 %	43.5–53.5 %
Ulnaris lateralis	lateral tuberosity of the radius	lateral styloid process of the radius - caudal side		36.5–53 %	18–23.5 % 35.5–47 %	31–62.5 %	36.5–47 %
Vastus lateralis	greater trochanter of the femur	tibial crest		45–55 %	31–50 %	45–60 %	45–50 %

seems an essential yet-to-be-solved issue in equine studies.

It is commonly indicated that surface EMGs should be detected over the muscle belly, midway between the tendinous areas and the innervation zone (Beretta Piccoli et al., 2014; Hermens et al., 2000; Rainoldi et al., 2000). Furthermore, electrode pairs should be placed in line with the muscle fibre direction, avoiding muscle borders, especially when studying dynamic contractions (Farina et al., 2004; Hermens et al., 2000). This would result in an optimal position for a pair of bipolar detection electrodes where the signal-to-noise ratio (SNR) is high, stride-to-stride variability is low, and the signal is most representative of the muscle.

This study aimed to start the development of recommendations for bipolar electrode locations to measure muscle activation in horses. These recommendations are meant for the group of users of surface EMG who focus their efforts on the equine locomotor apparatus. We used linear arrays of surface electrodes to investigate the effect of electrode location on surface EMGs in horses. The scope is limited to 21 superficial muscles and three Warmblood horses and should be considered as a starting point in our effort to improve the reproducibility of surface EMG study results.

2. Materials and methods

2.1. Horses

A convenience sample of three Dutch Warmblood horses (range values: age 12–14 years; body mass 545–611 kg; female) was included in this study. The horses were deemed sound by an experienced veterinarian (FSB) and had no known background with neurological disorders. The horses were regularly exercised and housed in boxes with daily turnout. All horses were exercised before the data collection period to allow acclimatisation to the treadmill (Bächi et al., 2018). Procedures were approved by the institutional animal welfare committee in compliance with the Dutch Act on Animal Experimentation.

2.2. Experimental protocol

The side of the horse on which the muscles were measured was randomly determined. The week before data collection, the horses were clipped, and ultrasound scans (Ultrasound machine: Epic 5, Philips, Eindhoven, The Netherlands; Transducer: L12-3 en C5-1 in musculoskeletal general pre-set) were performed on the selected muscles (Table 1) by a specialist from the European College of Veterinary Diagnostic Imaging (TR). This procedure allowed us to locate the muscle borders, tendinous areas and muscle fibre direction, which were marked on the skin by shaving thin lines.

Each horse went through six trials, with a maximum of two per day, where a different set of muscles was measured during each trial. For each trial, horses were exercised on a treadmill (Mustang 2200, Kagra AG, Fahrwangen, Switzerland) and underwent a 5-minute warm-up period at walk (6.0–6.5 km/h). Afterwards, the transition to trot was made (12.5–13.5 km/h, depending on individual gait stability). When the horse reached a stable trot, the measurement was started and data were collected for 60 s per trial.

2.3. Electrode placement and data recording

For each muscle, specific anatomical landmarks were selected to aid in the placement of the electrodes. Specifically, similar to SENIAM guidelines (Hermens et al., 2000), two anatomical landmarks on opposite sides of the muscle were chosen, such that a straight line between them would parallel the muscle fibre direction, and the line would fall approximately equidistant between both marked muscle borders. The distance between these anatomical landmarks was measured using a standard measuring tape and rounded to half centimetres. Then, the 50 % point between these anatomical landmarks was marked for each

muscle. Care was taken that the horse was standing square with a neutral head and neck position for this whole procedure. An overview of the anatomical landmarks chosen for each muscle is shown in Fig. 1.

Prior to applying the electrodes, the skin was clipped (0.5 mm hair length) and thoroughly cleaned (ethanol 80 %). Electrodes (pre-gelled Ag/AgCl; 3 mm diameter electrode; 24 mm inter-electrode distance; Cardinal Health, Waukegan, USA) were arranged into an array with a length depending on muscle size. Care was taken to ensure that two electrodes were positioned on either side of the 50 % mark. When this was not possible, one electrode was placed on the 50 % mark. Then, electrodes were placed adjacent to each other, along the muscle fibre direction, until we reached the muscle borders or the tendinous areas we determined with ultrasound scans. The ground electrode was positioned over either the tip of the spina scapula or the tuber coxae on the measured side. Tiny drops of mastix-based skin glue were used to fix the electrodes on the skin.

Surface EMG data were collected in monopolar derivation (referred to the average reference) and pre-amplified, sampled at 4000 Hz and A/D converted with 24-bit resolution (SAGA, TMSi, Oldenzaal, the Netherlands). The cables were arranged in a way to minimise pull on the electrodes when the horse was moving and attached to the horse using animal polster (supplementary Fig. 1). Before the measurement was started, electrode-skin impedance levels were checked using a built-in function of the measuring equipment to control for improper electrode adhesion. In addition, kinematic data were collected using ten inertial measurement units (IMU; ProMove-Mini, Inertia Technology B.V., Enschede, The Netherlands) sampling at 200 Hz, to allow segmentation of strides. The IMUs were placed on the head, withers, pelvis, tubera coxae, and the lateral aspects of the four lower limbs of the horse. An additional IMU was mounted on the surface EMG equipment, which also has an embedded three-dimensional (3D) accelerometer sampling at 4000 Hz, in order to synchronise the surface EMG and kinematic data.

2.4. Data analysis

All data analyses were performed in MATLAB (2022b, MathWorks, Natick, USA), and an overview of the data analysis procedure is illustrated in Fig. 2.

Surface EMG and kinematic signals were synchronised using a cross-correlation algorithm based on the dimensionless Euclidean norm of the 3D acceleration signals of the embedded accelerometer of the surface EMG equipment and the IMU mounted on top of it. The accelerometric signals from the surface EMG equipment were down-sampled to match the sampling frequency of the IMU system.

First, channels with extreme values were removed (Rojas-Martínez et al., 2012). Then, single-differential surface EMG signals were computed in the proximal-distal or cranial-caudal direction as the difference between two monopolar signals recorded from adjacent electrodes. Double-differential signals were computed similarly from the single-differential signals. Spectral analysis was performed in order to check for the presence of powerline interference. The single- and double-differential signals were bandpass filtered with a 4th order Butterworth filter (zero-lag; 40–450 Hz cut-off frequencies (St. George et al., 2018)).

To determine if some activation bursts may have originated from sources other than the targeted muscle (i.e., crosstalk), double- and single-differential signals were stride segmented and time-normalised from measured-side hind hoof impact to the following hoof impact from the same limb. Subsequently the double-differential and two single-differentials were plotted and qualitatively compared (Vieira and Botter, 2021). When an additional burst was visible in one or both of the single-differential signals, but not in the double-differential signal, these single-differential channels were classified as channels with suspected crosstalk.

For each single-differential signal, the signal-to-noise ratio (SNR) and coefficient of variation (CoV) were computed over ten strides (Yaserifar and Souza Oliveira, 2022). For the SNR computation, for each muscle

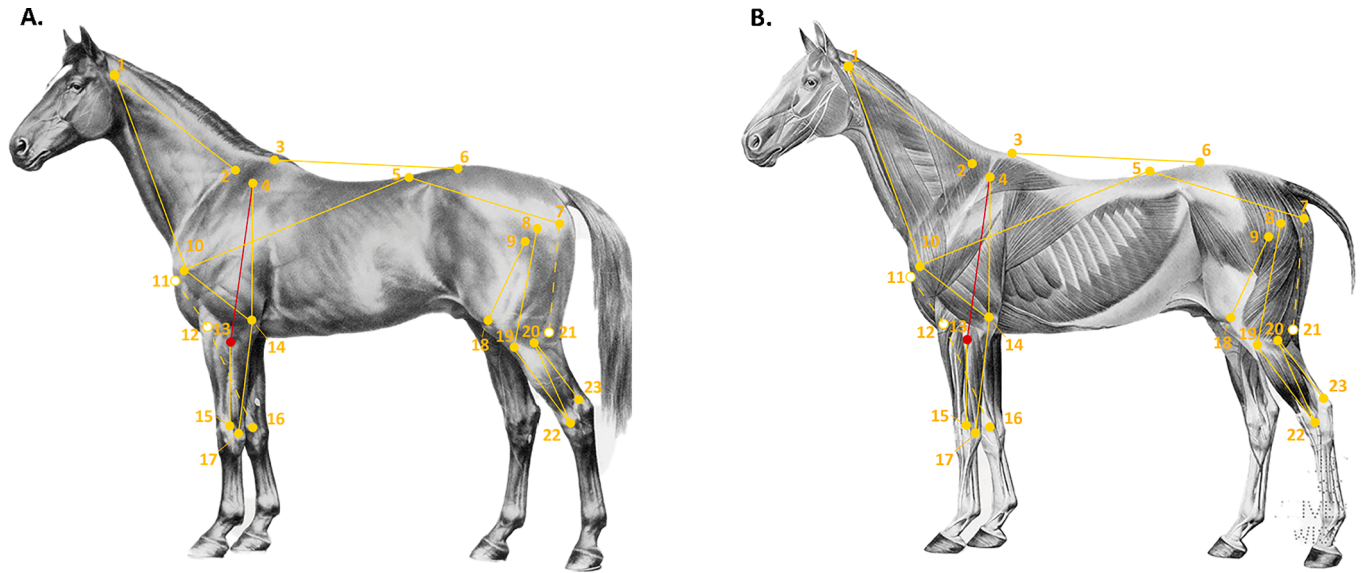


Fig. 1. Anatomical landmarks and reference lines used from the skin surface (A) and over the muscles (B). The numbers indicate the anatomical landmarks as follows: (1) wing of the atlas; (2) cranial angle of the scapula; (3) withers, T6; (4) proximal tip of the spina scapula; (5) proc. spinosus of lumbar vertebra 4; (6) tubera sacrale; (7) tuber ischiadicus; (8) caudal part of the greater trochanter of the femur; (9) cranial part of the greater trochanter of the femur; (10) cranial part of the greater tuberosity of the humerus; (11) manubrium of the sternum; (12) lacerus fibrosus; (13) lateral side of the caput radii/tuberositas radialis; (14) olecranon; (15) lateral styloid process of the radius - ventral side; (16) medial styloid process of the radius; (17) lateral styloid process of the radius - caudal side; (18) tibial crest; (19) lateral tibial condyle and head of the fibula; (20) lateral tibial condyle and head of the fibula; (21) at the height of the insertion of the m. gracilis; (22) lateral ridge of trochlea of talus; (23) calcaneal tubor. The lines represent the reference lines used for all muscles included in this study. The red line (between anatomical landmarks 4 and 13) represents a reference line that was chosen for the m. deltoideus, which was excluded. The illustrations were adapted from 'Handbuch der Anatomie der Tiere für Künstler' (Ellenberger and Davis, 2013). (For interpretation of the references to colour in this figure legend, the reader is referred to the web version of this article.)

and horse, ten segments of noise (no activity burst) and signals (activity burst) were manually selected by an experienced evaluator (IHS, for an example, see [supplementary Fig. 2](#)) for all single-differential signals of a muscle simultaneously. The signal-to-noise ratio in dB was then approximated as follows:

$$SNR_{i,n} = 10 \cdot \log_{10} \frac{rms(signal\ segment_{i,n})^2}{rms(noise\ segment_{i,n})^2} \quad (1)$$

Where i is the i^{th} extracted segment and n the n^{th} channel. The ten SNR values were then averaged to obtain one value per channel n of each muscle and horse. Finally, single-differential channels in the array with SNR greater than or equal to 70 % of the maximum value were considered for further analysis and are hereafter called the 'selected channels'.

For the CoV computation, the single-differential signals were rectified, low pass filtered (4th order Butterworth filter, zero-lag; 25 Hz cut-off frequency) to obtain the envelope of the signal (Clancy et al., 2023) and time-normalised from measured-side hind hoof impact to the following hoof impact of the same limb (101 data samples over a complete stride, 0–100 %). After that, the mean and standard deviation were calculated for each point of the time-normalised stride. Then, for each the CoV was calculated for each channel n as follows:

$$\mu_n(t) = \frac{1}{S} \sum_{s=1}^S x_s(t) \quad (2)$$

$$\sigma_n(t) = \sqrt{\frac{1}{S} \sum_{s=1}^S (x_s(t) - \mu_n(t))^2} \quad (3)$$

$$CoV_n = 100 \cdot \frac{1}{T} \sum_{t=1}^T \frac{\sigma_n(t)}{\mu_n(t)} \quad (4)$$

Where x is the time and amplitude normalised EMG signal over T samples and S is the number of strides. Equations (2) and (3) describe

how the mean value μ and the standard deviation σ were calculated at time normalised t over all S stride signals x . Finally, the CoV in % was computed as the mean ratio of σ and μ , as described in (4).

This provided N values for each muscle (where N is the number of available channels, equal to the length of the electrode array minus 1), which describe the distribution CoV over the array per muscle per horse. The CoV was evaluated to assess the within muscle repeatability and is expressed in percentage (%). In addition, in order to compare with other studies, we computed the CoV with the method proposed by Winter et al. (Winter, 1983) and the variance ratio (Hershler and Milner, 1978) on both the non-normalised and amplitude normalised surface EMG signals (Burden et al., 2003). These results can be found in [supplementary table 1](#).

2.5. Safe zone determination

To control for between-subject variability in muscle size, the longitudinal locations of the electrodes were expressed as a percentage of the distance between the anatomical landmarks used for electrode placement. Then, the locations of the selected channels were noted for all horses and muscles. Adjacent selected channels were considered as a 'safe zone' for each individual muscle. The proximal/cranial and distal/caudal extents of these zones were reported, where we allowed for the possibility of having multiple of these zones within a muscle. We consider these zones the 'safe zones' for measuring that muscles' activity. In order to determine the common safe zone between horses, the overlap of the safe zones of the individual horses was reported. These areas within the overlapping safe zones may be considered for the standardisation of electrode location.

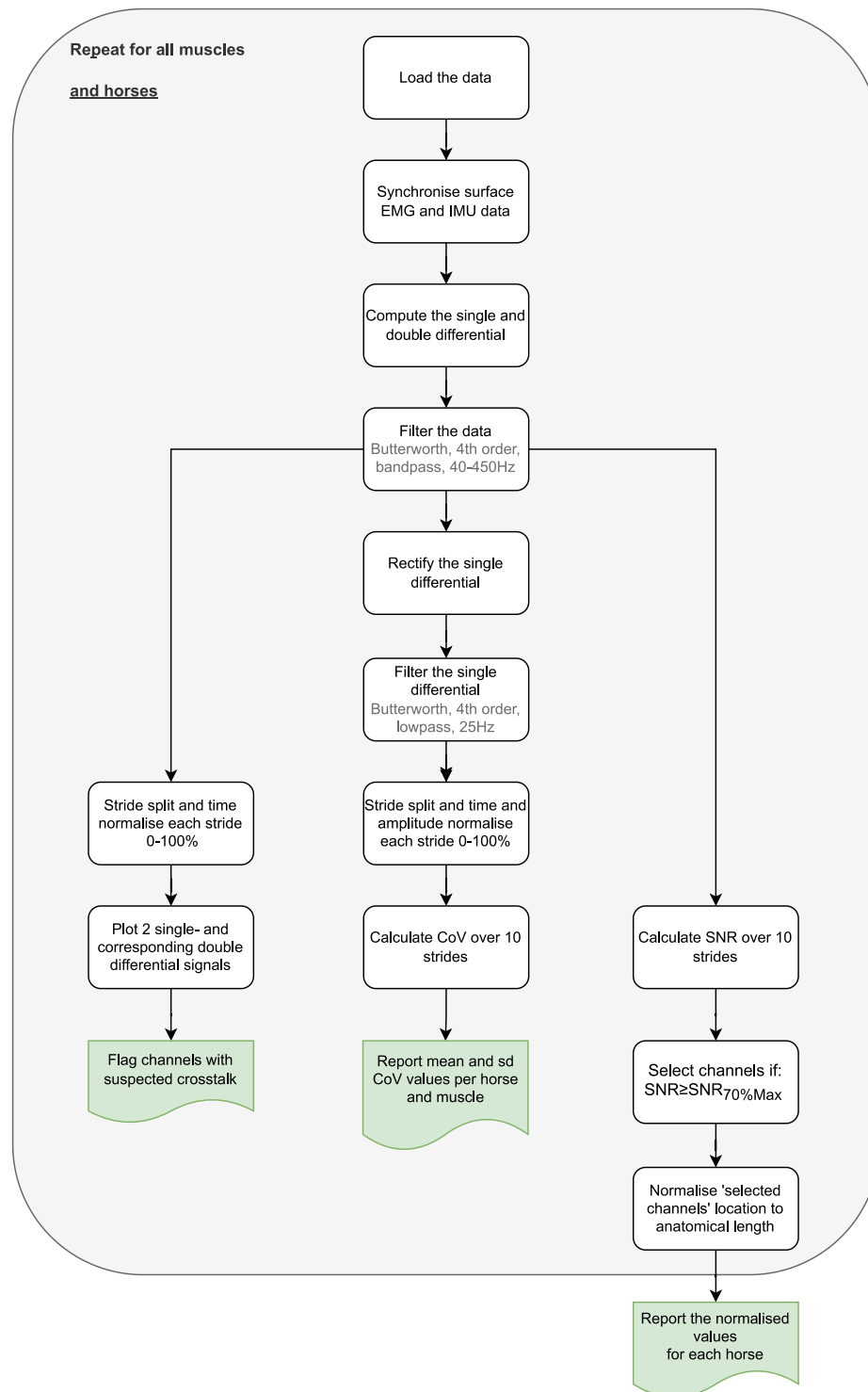


Fig. 2. Flow diagram of the data analysis. Rectangle blocks represent the individual steps and green blocks indicate outputs. All steps within the grey rectangle were repeated for all muscles and horses. Electromyography (EMG); inertial measurement unit (IMU); coefficient of variation (CoV); signal-to-noise ratio (SNR). (For interpretation of the references to colour in this figure legend, the reader is referred to the web version of this article.)

3. Results

3.1. General description

All horses performed the six trials without difficulties (mean \pm sd strides per trial = 76.8 ± 4.7). In two horses, muscles were measured on their left side, in the other horse, on the right side. For the m. deltoideus, the chosen reference line was inappropriate as it did not fall equidistant

between the muscle borders nor in parallel with the muscle fibre direction (Fig. 1), therefore all channels were excluded for this muscle. In addition, the data from the m. gluteus medius was lost for horse 1 due to poor electrode-skin contact. No powerline interference was found in any of the signals based on spectral analysis. For the final dataset, 423/449 channels were included for further analysis (supplementary table 2).

3.2. Spatial localisation of the SNR and CoV distribution

For most muscles and horses, the highest SNR values were found in the channels cranial or proximal to the 50 % marks (Table 1). There were clear differences between channels for most muscles in terms of SNR and the qualitative signal assessment (Fig. 3). Differences were observed between subjects for some muscles, mainly in the m. extensor carpi radialis and m. flexor digitorum profundus (Table 1). For these muscles, there were no overlapping safe zones between horses where SNR values were equal to, or larger than 70 % of the maximum value (Fig. 4).

In general, CoV values differed between locations, muscles and horses and varied between 29.3 % and 96.0 % with a mean \pm sd of 44.8 ± 10.1 %. To give an impression of the differences within a muscle between horses, mean and sd per muscle and horse are given in Table 2. In addition, the CoV values, as well as the SNR values and the other

measures of variability, for all tested locations and muscles were presented in supplementary table 1. A representative example of the differences within a muscle and between two horses is given in Fig. 5.

3.3. Single- vs double differential signals

In a few signals from some muscles crosstalk was suspected. For three muscles, crosstalk was suspected for more than one horse. These were the m. Brachiocephalicus (horse 2 and horse 3; Fig. 6), m. Semitendinosus (horse 1 and horse 2) and m. longissimus (horse 1 and horse 3). Other muscles where crosstalk was suspected were m. extensor digitorum lateralis and m. triceps brachii caput laterale for horse 1; m. extensor digitorum longus and m. latissimus dorsi for horse 2 and m. extensor digitorum communis, m. pectoralis pars descendens and m. vastus lateralis for horse 3. For these muscles not all signals were suspected to contain crosstalk, only those from the channels at the ends of

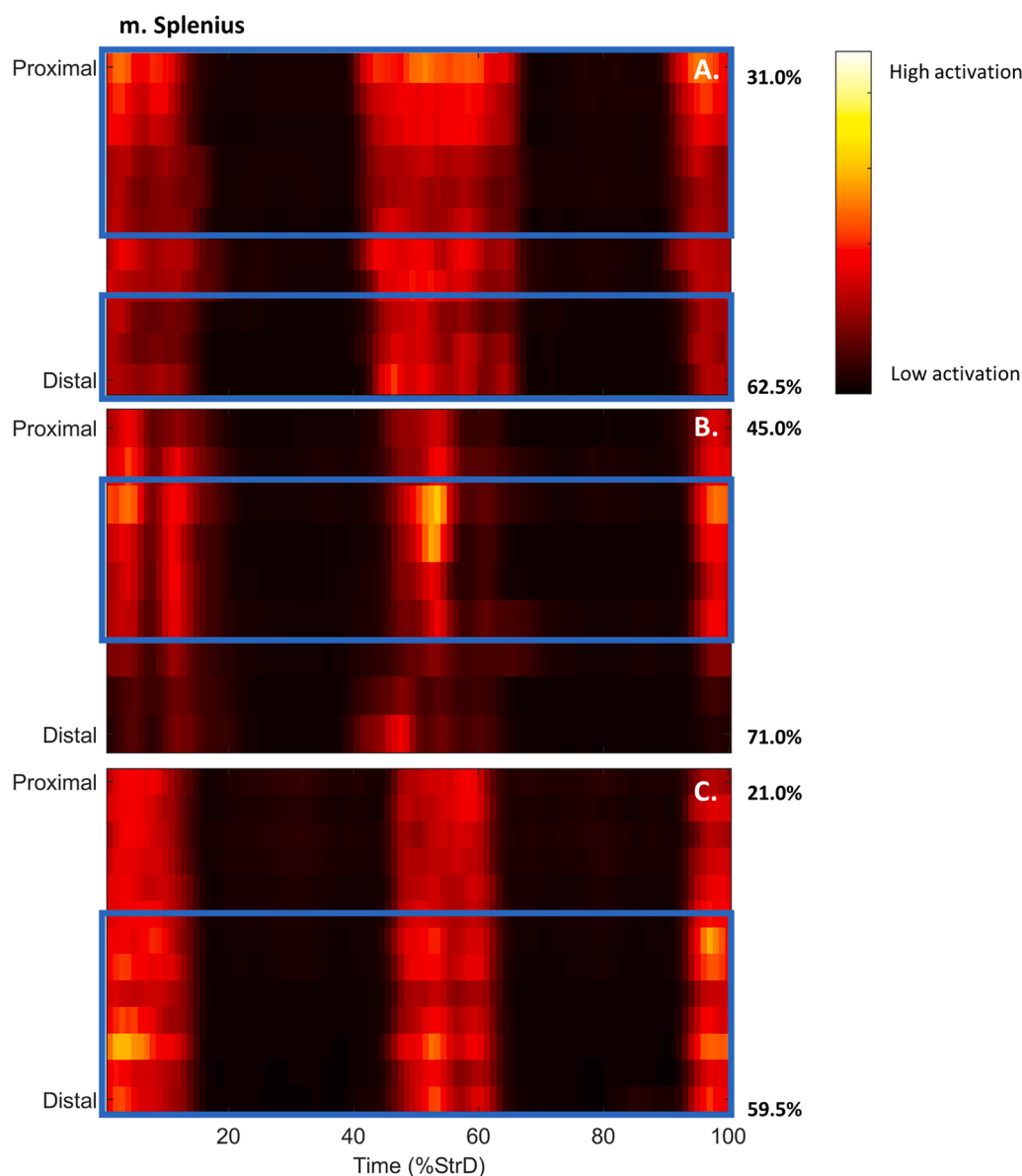


Fig. 3. An example of the differences between horses with one or two overlapping safe zones for the m. splenius. Each row in a sub-panel represents the mean and time-normalised activation pattern from a channel. The top row shows the most proximal channel and the bottom row the most distal channel for that horse. On the right side of the panel the corresponding location of that channel is given as a percentage between the anatomical landmarks used. The blue boxes indicate the selected channels. The colour scale gives an estimate of the amplitude, where the brighter colours represent the higher voltages. Activation patterns are shown for horse 1 (A), horse 2 (B) and horse 3 (C). (For interpretation of the references to colour in this figure legend, the reader is referred to the web version of this article.)

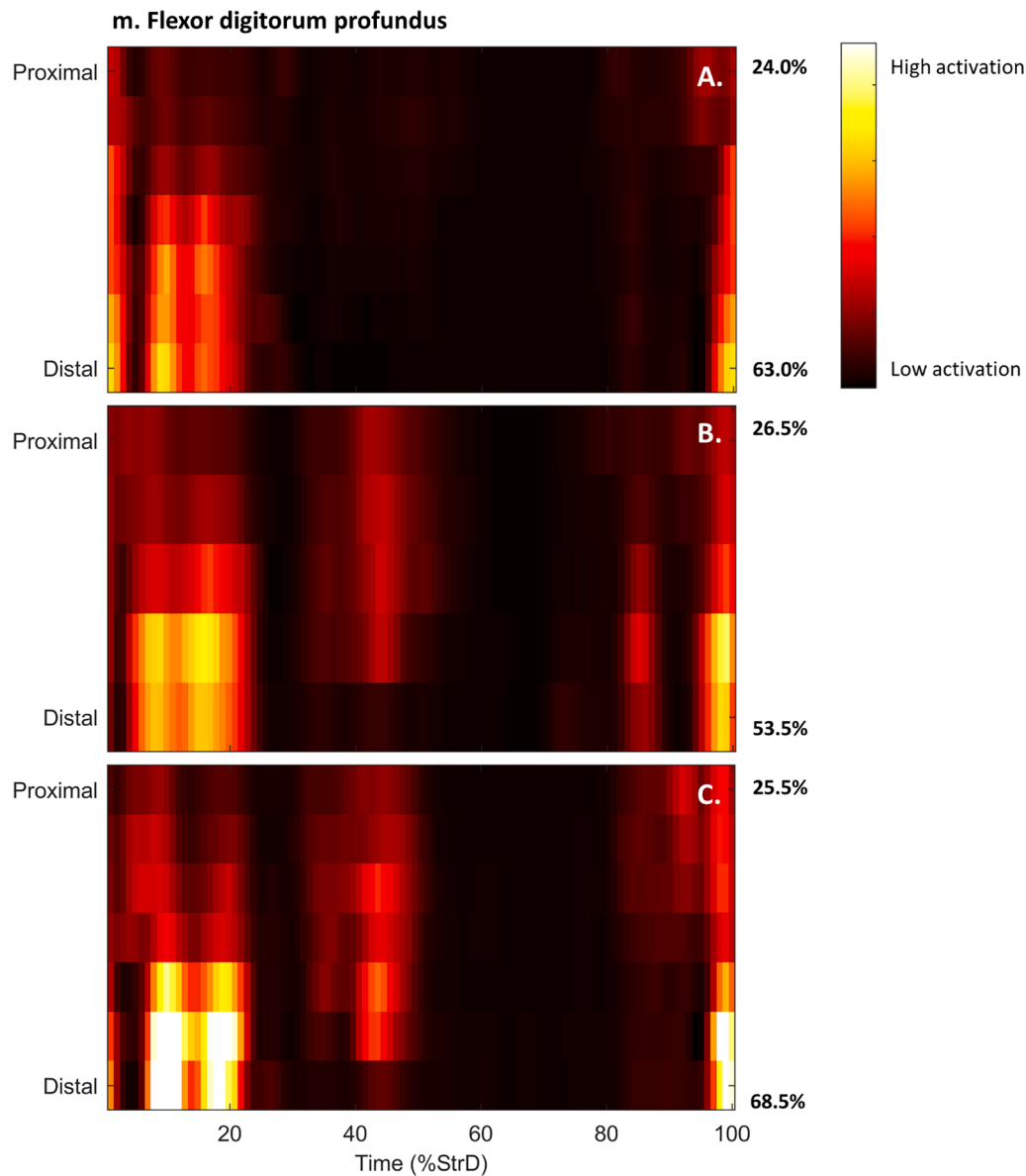


Fig. 4. An example of the differences between horses with no overlapping safe zone for the m. flexor digitorum profundus. Each row in a sub-panel represents the mean and time-normalised activation pattern from a channel. The top row shows the most proximal channel and the bottom row the most distal channel for that horse. On the right side of the panel the corresponding location of that channel is given as a percentage between the anatomical landmarks used. The colour scale gives an estimate of the amplitude in μV , where the brighter colours represent the higher voltages. Activation patterns are shown for horse 1 (A), horse 2 (B) and horse 3 (C).

the arrays.

4. Discussion

The challenge of choosing electrode locations for surface EMG recordings in horses is essential for many fields, ranging from basic research to clinical applications. Despite the increasing number of studies involving surface EMG in horses, there is a substantial discrepancy or unclarity regarding the used electrode locations (Valentin and Zsoldos, 2017). Here, we addressed this issue by investigating the signal quality for twenty muscles in three horses using electrode arrays. We demonstrated that, for most muscles and horses, the highest SNR values were detected near or cranial/proximal to the central region of the muscle. There were larger differences in CoV values between muscles and horses than within muscles. The current results may provide initial recommendations for choosing electrode locations to collect surface EMG data from horses.

It is commonly indicated that to measure reliable surface EMG signals, detection electrodes need to be placed between the innervation zone and tendinous areas and during the motion the detection electrodes should not move over either of these zones (Farina, 2006; Farina et al., 2004; Hermens et al., 2000; Rainoldi et al., 2004, 2000). In the current study, tendinous areas were determined using ultrasound scans. The innervation zones are usually identified by having the test subject perform isometric contractions while measured using grids or arrays of electrodes (Barbero et al., 2012; Masuda and Sadoyama, 1991; Merletti et al., 2003; Nishihara et al., 2010; Rainoldi et al., 2000) or by electrical stimulation (Huang et al., 2019). The maximal shift in innervation zone location during the motion cycle can then be determined by performing isometric contractions at the extremes of the motion cycle (Rainoldi et al., 2004; Sacco et al., 2009). However, this is impossible when studying horses, as we cannot ask the subject to perform a specific task. We were limited to a locomotion task, in this case trotting, which was standardised in speed by having the horses trot on a treadmill. It was

Table 2

Mean and standard deviation (sd) of the coefficient of variation (CoV; %) per muscle and horse.

Muscle	Horse		
	Horse 1	Horse 2	Horse 3
Biceps femoris	39.1 ± 2.8	43.2 ± 3.8	41.6 ± 8
Brachiocephalicus	44.6 ± 2.5	53 ± 6.8	41.8 ± 1.3
Extensor digitorum communis	48.2 ± 4.2	44.6 ± 1.3	37.1 ± 3.6
Extensor carpi radialis	58.6 ± 4.9	50.7 ± 2.8	45.9 ± 4.1
Extensor digitorum lateralis	44.8 ± 2.9	36.1 ± 2	35.9 ± 4.2
Extensor digitorum longus	45.9 ± 4.5	40.4 ± 2.7	37.1 ± 3
Flexor carpi ulnaris	39.1 ± 1.8	41.9 ± 2.2	53.9 ± 5.5
Flexor digitorum profundus	42.6 ± 6.8	51.1 ± 6.4	32.8 ± 7.9
Gluteus medius		48.5 ± 5.7	38.3 ± 7.3
Latissimus dorsi		30.2 ± 1.5	
Longissimus	31.5 ± 2.2	50.9 ± 4.8	41.5 ± 3.8
Pectoralis pars descendens	56.2 ± 7.2	49.7 ± 6.5	39.8 ± 4
Pectoralis pars ascendens	41.6 ± 12.3	40.3 ± 3.8	40.5 ± 2.2
Rectus abdominis	71.1 ± 13.4	92.2 ± 2.5	48.8 ± 20.3
Semitendinosus	48 ± 18.9	56.4 ± 4.8	35.3 ± 2.1
Splenius	42.8 ± 3.1	43.2 ± 2.6	44.8 ± 3.2
Triceps brachii, caput laterale	47.8 ± 2.5	50.3 ± 2.1	43.3 ± 7.2
Triceps brachii caput longum	34.4 ± 1.7	40.2 ± 1.1	37.8 ± 4.5
Ulnaris lateralis	42.8 ± 2.3	42.9 ± 3.6	56.5 ± 5.2
Vastus lateralis	41.1 ± 3	39.6 ± 3.3	43.2 ± 4.4

therefore impossible to reliably quantify specific parameters indicative of the presence of innervation zones, especially since we do not know the degree of muscle lengthening and shortening during the gait cycle in the horse, and skin displacement can be substantial (van Weeren et al., 1990). Therefore, we did not include any parameters indicative of innervation zones, and our considerations are solely based on SNR values within a muscle during trot.

The CoV was used to evaluate the intra-location (within muscle and horse) reliability of the surface EMG profiles. Even though CoV values did not greatly differ between the locations within most muscles, variability was still relatively high for some muscles, despite the horses being trotted at a stable speed on a treadmill. The variability was highest for bi-articular muscles, such as the m. semitendinosus or the m. triceps brachii caput longum, and the m. rectus abdominis. This was to be expected for the bi-articular muscles and in agreement with a recent study

on the reliability and repeatability of surface EMG in horses (St. George et al., 2023) and during walking and running in humans (Elsais et al., 2020; Kadaba et al., 1989; Karamanidis et al., 2004). In addition, the bi-articular muscles also showed larger differences between locations, as can be found in the [supplementary material](#). We know different methods are used to determine the degree of variability in surface EMG signals, and the CoV is sensitive to the method of amplitude normalisation. We did not amplitude normalise our data, and comparisons were only made within horse and muscle. Other measures such as the variance ratio, which can be found in the [supplementary table S1](#), may be worth investigating to assess the variability of surface EMG signals in horses. This measure is independent of which normalisation method is used (Burden et al., 2003) and the number of analysed strides (Gabel and Brand, 1994). The last being of high importance, as it may be challenging to get enough repetitions of the same task when working with animals.

Differences were subjectively observed between muscles in terms of the consistency of the activation pattern across the different channels. In voluntary dynamic contractions, as is the case during locomotion tasks, activity seems to be distributed more heterogeneously within pennate muscles in humans (Kinugasa et al., 2005; McLean and Goudy, 2004). This may explain why, for more fusiform muscles, for instance the m. biceps femoris, channels seemed very similar to each other in terms of activation pattern and timing, while for other more pennate muscles, for instance the m. flexor digitorum profundus (Payne et al., 2005), the activation pattern varied more between different channels. This could mean that for pennate muscles, multiple electrode locations would need to be used when aiming to describe the whole muscle activation pattern.

For the m. extensor carpi radialis and the m. flexor digitorum profundus, there was no overlap in safe zones between horses. This might be due to the differences in innervation zone locations between individuals, as it is known that innervation zones differ in location in human muscles (An et al., 2010; Beretta Piccoli et al., 2014; Sacco et al., 2009). Furthermore, the muscles where no overlapping safe zones were found were both distal limb muscles. These muscles are generally smaller in size, their architecture is more pennate, and they have longer tendons relative to the muscle size. Therefore, we could place arrays with fewer electrodes on these muscles; hence, it was not surprising to find smaller

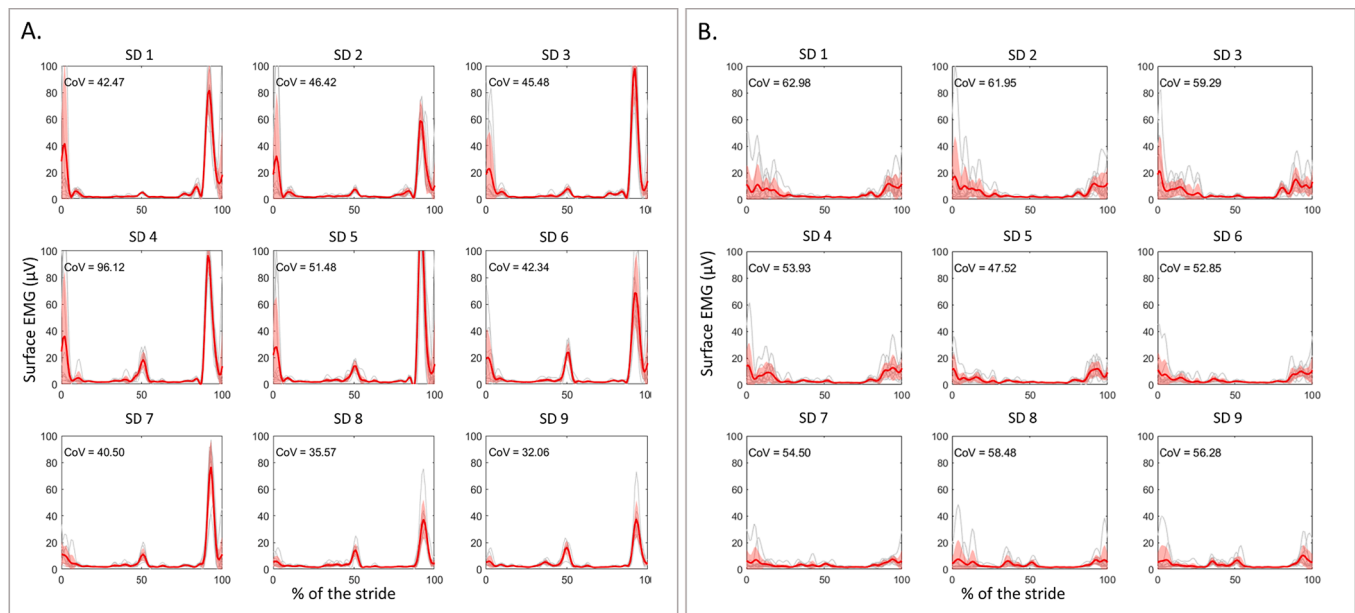


Fig. 5. Two examples for the inter-muscle surface EMG profiles from the m. semitendinosus. The mean (solid red) and standard deviation (shaded area) of the time-normalised (ten strides) surface EMG data (grey; in micro volts (µV)) of the m. semitendinosus of horse 1 (A) and horse 2 (B). Every subpanel shows the data of one location from the most proximal single differential (SD 1) to the most distal single differential (SD 9). The coefficient of variation (CoV) is indicated for every location. (For interpretation of the references to colour in this figure legend, the reader is referred to the web version of this article.)

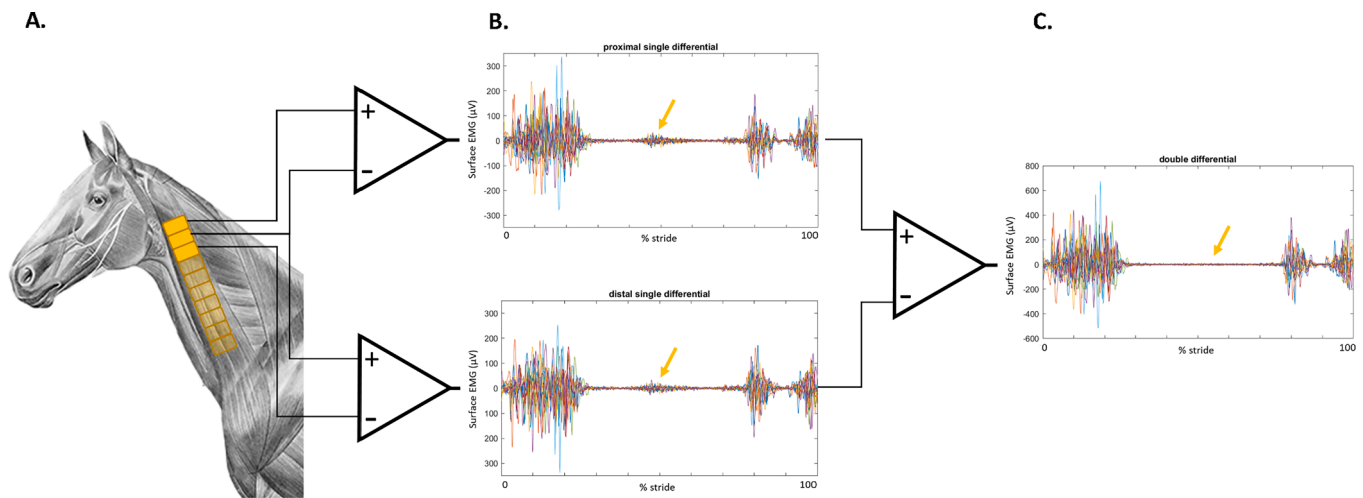


Fig. 6. An example of the comparison between single and double differential signals with suspected crosstalk of the m. brachiocephalicus. A schematic overview of the brachiocephalic muscle and the electrode array (A), where solid rectangles represent the electrodes from which the signals were compared. Each line represents a time-normalised stride single differential signal (B) and double differential signal (C) from the m. brachiocephalicus of horse 3. The arrows indicate the activation burst that is suspected to be crosstalk. These bursts are visible in the single differential signals, but not in the double differential signals. Note that the squares do not represent actual electrode size.

or no overlapping safe zones. In addition, due to conformational differences between horses, it was not always possible to place arrays with a similar length on each horse. For instance, on horse 1, we could not place electrodes further than the 53.5 % point on the m. flexor digitorum profundus, where on the other horses we could place electrodes up to up to 63 % and 68.5 % of the distance between the anatomical landmarks. Still, the SNR was highest for the more distally located channels of horse 1, similar to the other two horses, where the normalised safe zones were also located more distally.

For this study, only a small and homogenous group of horses was included. Extrapolating our findings to the entire equine population must therefore be done with caution. Moreover, even in this small homogenous sample, large differences between horses were found for some muscles. It is known that innervation zone locations differ between humans (Barbero et al., 2012; Saitou et al., 2000), and the SENIAM recommendations do not always lead to the most optimal electrode position for all individuals (Sacco et al., 2009). This stresses the importance of choosing the correct electrode configuration to fit the aims of individual studies. Based on our findings, we propose that the bipolar electrode positions within the safe zones found in this study might be sufficient to determine muscle onset and offset during gait tasks. However, especially for non-parallel or fusiform muscles and questions related to activation distribution over a muscle, the proposed locations alone might not be sufficient and multiple sets of detection electrodes or grids might be required.

With this project, a first effort was made to standardise bipolar electrode locations in horses. We believe this will aid the reliability of surface EMG measures in horses and can be seen as a step towards clinical applications, such as aiding lameness diagnostics, exercise selection for rehabilitation purposes and monitoring treatment. The recommended locations, i.e. locations in the common safe zone of a muscle, of this study should be considered as a starting point and so far they only concern the locations for bipolar measurements during dynamic tasks. The recommendations provided will change over time as new empirical evidence emerges and new technologies to record surface EMGs are developed. Advances in technology, such as the development of new types of electrodes (e.g. high adhesion stretchable electrodes (Lee et al., 2023; Liu et al., 2018), screen-printed electrodes (Spanu et al., 2021) or electrodes integrated in textiles (Etana et al., 2023; Isezaki et al., 2019), will provide solutions that allow for approximation of muscle activation in the horse in a more natural way. We foresee that the

recommendations must be updated accordingly. Further efforts must be made to continue the standardisation of surface EMG measurements in horses and other species. Examples are: (1) how to prepare greasy and densely hairy skin for reliable surface EMG recordings; (2) Where to place electrodes to measure muscles that were not included in this study or where to place grids for high-definition surface EMG measurements and (3) how to process the signals, for instance in terms of normalisation procedures to compare between individuals and the number of strides needed to draw reliable conclusions. This will require the combined effort of experts in the field, and we sincerely hope that the community will contribute to this in the near future.

Funding

This research did not receive any specific grant from funding agencies in the public, commercial, or not-for-profit sectors.

CRediT authorship contribution statement

I.H. Smit: Writing – review & editing, Writing – original draft, Visualization, Methodology, Investigation, Formal analysis, Data curation, Conceptualization. **J.I.M. Parmentier:** Writing – review & editing, Writing – original draft, Visualization, Methodology, Formal analysis, Data curation. **T. Rovel:** Writing – original draft. **J. van Dieen:** Writing – review & editing, Methodology. **F.M. Serra Bragança:** Writing – review & editing, Supervision, Methodology, Funding acquisition, Conceptualization.

Declaration of competing interest

The authors declare that they have no known competing financial interests or personal relationships that could have appeared to influence the work reported in this paper.

Acknowledgements

The authors would like to thank the Rhana Aarts, Tijn Spoormakers, students and animal caretakers for their help with the data collection.

Appendix A. Supplementary data

Supplementary data to this article can be found online at <https://doi.org/10.1016/j.jelekin.2024.102884>.

References

- An, X.C., Lee, J.H., Im, S., Lee, M.S., Hwang, K., Kim, H.W., Han, S.H., 2010. Anatomic localization of motor entry points and intramuscular nerve endings in the hamstring muscles. *Surg. Radiol. Anat.* 32, 529–537. <https://doi.org/10.1007/s00276-009-0609-5>.
- Bächli, B., Wiestner, T., Stoll, A., Waldern, N.M., Imboden, I., Weishaupt, M.A., 2018. Changes of ground reaction force and timing variables in the course of habituation of horses to the treadmill. *J. Equine Vet. Sci.* 63, 13–23. <https://doi.org/10.1016/j.jevs.2017.12.013>.
- Barbero, M., Merletti, R., Rainoldi, A., 2012. *Atlas of Muscle Innervation Zones: Understanding Surface Electromyography and its Applications*. Springer, Milan.
- Beretta Piccoli, M., Rainoldi, A., Heitz, C., Wüthrich, M., Boccia, G., Tomasani, E., Spirolazzi, C., Egloff, M., Barbero, M., 2014. Innervation zone locations in 43 superficial muscles: toward a standardization of electrode positioning. *Muscle Nerve* 49, 413–421. <https://doi.org/10.1002/mus.23934>.
- Besomi, M., Hodges, P.W., Van Dieën, J., Carson, R.G., Clancy, E.A., Disselhorst-Klug, C., Holobar, A., Hug, F., Kiernan, M.C., Lowery, M., McGill, K., Merletti, R., Perreault, E., Søgaard, K., Tucker, K., Besier, T., Enoka, R., Falla, D., Farina, D., Gandevia, S., Rothwell, J.C., Vicenzino, B., Wrigley, T., 2019. Consensus for experimental design in electromyography (CEDE) project: electrode selection matrix. *J. Electromyogr. Kinesiol.* 48, 128–144. <https://doi.org/10.1016/j.jelekin.2019.07.008>.
- Besomi, M., Hodges, P.W., Clancy, E.A., Van Dieën, J., Hug, F., Lowery, M., Merletti, R., Søgaard, K., Wrigley, T., Besier, T., Carson, R.G., Disselhorst-Klug, C., Enoka, R.M., Falla, D., Farina, D., Gandevia, S., Holobar, A., Kiernan, M.C., McGill, K., Perreault, E., Rothwell, J.C., Tucker, K., 2020. Consensus for experimental design in electromyography (CEDE) project: amplitude normalization matrix. *J. Electromyogr. Kinesiol.* 53, 102438. <https://doi.org/10.1016/j.jelekin.2020.102438>.
- Bragança, F.M.S., Rhodin, M., Weeren, P.R.V., 2018. On the brink of daily clinical application of objective gait analysis: what evidence do we have so far from studies using an induced lameness model? *Vet. J.* 234, 11–23. <https://doi.org/10.1016/j.tvjl.2018.01.006>.
- Burden, A.M., Trew, M., Baltzopoulos, V., 2003. Normalisation of gait EMGs: a re-examination. *J. Electromyogr. Kinesiol.* 13, 519–532. [https://doi.org/10.1016/S1050-6411\(03\)00082-8](https://doi.org/10.1016/S1050-6411(03)00082-8).
- Clancy, E.A., Morin, E.L., Hajian, G., Merletti, R., 2023. Tutorial. Surface electromyogram (sEMG) amplitude estimation: best practices. *J. Electromyogr. Kinesiol.* 72, 102807. <https://doi.org/10.1016/j.jelekin.2023.102807>.
- De Luca, C.J., 1997. The use of surface electromyography in biomechanics. *J. Appl. Biomech.* 13, 135–163. <https://doi.org/10.1123/jab.13.2.135>.
- Ellenberger, W., Davis, F.A., 2013. *An atlas of animal anatomy for artists*. Dover Publications.
- Elsais, W.M., Preece, S.J., Jones, R.K., Herrington, L., 2020. Between-day repeatability of lower limb EMG measurement during running and walking. *J. Electromyogr. Kinesiol.* 55, 102473. <https://doi.org/10.1016/j.jelekin.2020.102473>.
- Etana, B.B., Malengier, B., Timothy, K., Wojciech, S., Krishnamoorthy, J., Van Langenhove, L., 2023. A review on the recent developments in design and integration of electromyography textile electrodes for biosignal monitoring. *J. Ind. Text.* 53. <https://doi.org/10.1177/15280837231175062>, 15280837231175062.
- Farina, D., 2006. Interpretation of the surface electromyogram in dynamic contractions. *Exerc. Sport Sci. Rev.* 34, 121–127. <https://doi.org/10.1249/00003677-200607000-00006>.
- Farina, D., Cescon, C., Merletti, R., 2002. Influence of anatomical, physical, and detection-system parameters on surface EMG. *Biol. Cybern.* 86, 445–456. <https://doi.org/10.1007/s00422-002-0309-2>.
- Farina, D., Pozzo, M., Merlo, E., Bottin, A., Merletti, R., 2004. Assessment of average muscle fiber conduction velocity from surface EMG signals during fatiguing dynamic contractions. *IEEE Trans. Biomed. Eng.* 51, 1383–1393. <https://doi.org/10.1109/TBME.2004.827556>.
- Gabel, R.H., Brand, R.A., 1994. The effects of signal conditioning on the statistical analyses of gait EMG. *Electroencephalogr. Clin. Neurophysiol. Potentials Sect.* 93, 188–201. [https://doi.org/10.1016/0168-5597\(94\)90040-X](https://doi.org/10.1016/0168-5597(94)90040-X).
- Hermens, H.J.H., Freriks, B., Dissel, C., Rau, G., 2000. Development of recommendations for SEMG sensors and sensor placement procedures. *Electromyogr. Kinesiol.* 810, 333–349. <https://doi.org/10.1007/s10750-015-2551-3>.
- Hershler, C., Milner, M., 1978. An optimality criterion for processing electromyographic (EMG) signals relating to human locomotion. *IEEE Trans. Biomed. Eng.* 25, 413–420. <https://doi.org/10.1109/TBME.1978.326338>.
- Huang, C., Klein, C.S., Meng, Z., Zhang, Y., Li, S., Zhou, P., 2019. Innervation zone distribution of the biceps brachii muscle examined using voluntary and electrically-evoked high-density surface EMG. *J. Neuroengineering Rehabil.* 16, 73. <https://doi.org/10.1186/s12984-019-0544-6>.
- Isezaki, T., Kadone, H., Nijima, A., Aoki, R., Watanabe, T., Kimura, T., Suzuki, K., 2019. Sock-type Wearable sensor for estimating lower leg muscle activity using distal EMG signals. *Sensors* 19, 1954. <https://doi.org/10.3390/s19081954>.
- Kadaba, M.P., Ramakrishnan, H.K., Wootten, M.E., Gainey, J., Gorton, G., Cochran, G.V. B., 1989. Repeatability of kinematic, kinetic, and electromyographic data in normal adult gait. *J. Orthop. Res.* 7, 849–860. <https://doi.org/10.1002/jor.1100070611>.
- Karamanidis, K., Arampatzis, A., Brüggemann, G.-P., 2004. Reproducibility of electromyography and ground reaction force during various running techniques. *Gait Posture* 19, 115–123. [https://doi.org/10.1016/S0966-6362\(03\)00040-7](https://doi.org/10.1016/S0966-6362(03)00040-7).
- Kinugasa, R., Kawakami, Y., Fukunaga, T., 2005. Muscle activation and its distribution within human triceps surae muscles. *J. Appl. Physiol.* 99, 1149–1156. <https://doi.org/10.1152/japplphysiol.01160.2004>.
- Komi, P.V., Linnamo, V., Silventoinen, P., Sillanpää, M., 2000. Force and EMG power spectrum during eccentric and concentric actions. *Med. Sci. Sports Exerc.* 32, 1757–1762. <https://doi.org/10.1097/00005768-200010000-00015>.
- Lee, H., Lee, S., Kim, J., Jung, H., Yoon, K.J., Gandla, S., Park, H., Kim, S., 2023. Stretchable array electromyography sensor with graph neural network for static and dynamic gestures recognition system. *Npj Flex. Electron.* 7, 20. <https://doi.org/10.1038/s41528-023-00246-3>.
- Liu, K., Yan, J., Liu, Y., Ye, M., 2018. Noninvasive estimation of joint moments with inertial sensor system for analysis of STS rehabilitation training. *J. Healthc. Eng.* 2018, 6570617. <https://doi.org/10.1155/2018/6570617>.
- Madeleine, P., Bajaj, P., Søgaard, K., Arendt-Nielsen, L., 2001. Mechanomyography and electromyography force relationships during concentric, isometric and eccentric contractions. *J. Electromyogr. Kinesiol.* 11, 113–121. [https://doi.org/10.1016/S1050-6411\(00\)00044-4](https://doi.org/10.1016/S1050-6411(00)00044-4).
- Masuda, T., Sadoyama, T., 1991. Distribution of innervation zones in the human biceps brachii. *J. Electromyogr. Kinesiol.* 1, 107–115. [https://doi.org/10.1016/1050-6411\(91\)90004-0](https://doi.org/10.1016/1050-6411(91)90004-0).
- McLean, L., Goudy, N., 2004. Neuromuscular response to sustained low-level muscle activation: within- and between-synergist substitution in the triceps surae muscles. *Eur. J. Appl. Physiol.* 91, 204–216. <https://doi.org/10.1007/s00421-003-0967-3>.
- Merletti, R., 1999. Standards for reporting EMG data. *J. Electromyogr. Kinesiol.* 38, I-II. [https://doi.org/10.1016/S1050-6411\(18\)30035-x](https://doi.org/10.1016/S1050-6411(18)30035-x).
- Merletti, R., Farina, D., Gazzoni, M., 2003. The linear electrode array: a useful tool with many applications. *J. Electromyogr. Kinesiol.* 13, 37–47. [https://doi.org/10.1016/S1050-6411\(02\)00082-2](https://doi.org/10.1016/S1050-6411(02)00082-2).
- Nakazawa, K., Kawakami, Y., Fukunaga, T., Yano, H., Miyashita, M., 1993. Differences in activation patterns in elbow flexor muscles during isometric, concentric and eccentric contractions. *Eur. J. Appl. Physiol.* 66, 214–220. <https://doi.org/10.1007/BF00235096>.
- Nishihara, K., Chiba, Y., Suzuki, Y., Moriyama, H., Kanemura, N., Ito, T., Takayanagi, K., Gomi, T., 2010. Effect of position of electrodes relative to the innervation zone on surface EMG. *J. Med. Eng. Technol.* 34, 141–147. <https://doi.org/10.3109/03091900903480754>.
- Payne, R.C., Veenman, P., Wilson, A.M., 2005. Erratum: the role of the extrinsic thoracic limb muscles in equine locomotion (journal of anatomy (2004)). *J. Anat.* 206, 193–204. <https://doi.org/10.1111/j.1469-7580.2005.00353.x>.
- Rainoldi, A., Nazzaro, M., Merletti, R., Farina, D., Caruso, I., Gaudenti, S., 2000. Geometrical factors in surface EMG of the vastus medialis and lateralis muscles. *J. Electromyogr. Kinesiol.* 10, 327–336. [https://doi.org/10.1016/S1050-6411\(00\)00024-9](https://doi.org/10.1016/S1050-6411(00)00024-9).
- Rainoldi, A., Melchiorri, G., Caruso, I., 2004. A method for positioning electrodes during surface EMG recordings in lower limb muscles. *J. Neurosci. Methods* 134, 37–43. <https://doi.org/10.1016/j.jneumeth.2003.10.014>.
- Rojas-Martínez, M., Mañanas, M.A., Alonso, J.F., 2012. High-density surface EMG maps from upper-arm and forearm muscles. *J. Neuroengineering Rehabil.* 9, 85. <https://doi.org/10.1186/1743-0003-9-85>.
- Sacco, I.C.N., Gomes, A.A., Otuzi, M.E., Pripas, D., Onodera, A.N., 2009. A method for better positioning bipolar electrodes for lower limb EMG recordings during dynamic contractions. *J. Neurosci. Methods* 180, 133–137. <https://doi.org/10.1016/j.jneumeth.2009.02.017>.
- Saitou, K., Masuda, T., Michikami, D., Kojima, R., Okada, M., 2000. Innervation zones of the upper and lower limb muscles estimated by using multichannel surface EMG. *J. Hum. Ergol. (Tokyo)* 29, 35–52.
- Spanu, A., Botter, A., Zedda, A., Cerone, G.L., Bonfiglio, A., Pani, D., 2021. Dynamic Surface electromyography using stretchable screen-printed textile electrodes. *IEEE Trans. Neural Syst. Rehabil. Eng.* 29, 1661–1668. <https://doi.org/10.1109/TNSRE.2021.3104972>.
- St. George, L., Hobbs, S.J., Richards, J., Sinclair, J., Holt, D., Roy, S.H., 2018. The effect of cut-off frequency when high-pass filtering equine sEMG signals during locomotion. *J. Electromyogr. Kinesiol.* 43, 28–40. <https://doi.org/10.1016/j.jelekin.2018.09.001>.
- St. George, L., Spoormakers, T.J.P., Roy, S.H., Hobbs, S.J., Clayton, H.M., Richards, J., Serra Bragança, F.M., 2023. Reliability of surface electromyographic (sEMG) measures of equine axial and appendicular muscles during overground trot. *PLOS One* 18, e0288664.
- Valentin, S., Zsoldos, R.R., 2017. Europe PMC Funders Group Surface electromyography in animals: A systematic review 167–183. DOI: 10.1016/j.jelekin.2015.12.005.
- van Weeren, P.R., Van den Bogert, A.J., Barneveld, A., 1990. A quantitative analysis of skin displacement in the trotting horse. *Equine Vet. J.* 22, 101–109. <https://doi.org/10.1111/j.2042-3306.1990.tb04745.x>.
- Vieira, T.M., Botter, A., 2021. The accurate assessment of muscle excitation requires the detection of multiple Surface electromyograms. *Exerc. Sport Sci. Rev.* 49, 23–34. <https://doi.org/10.1249/JES.0000000000000240>.
- Winter, D.A., 1983. Biomechanical motor patterns in Normal walking. *J. Mot. Behav.* 15, 302–330. <https://doi.org/10.1080/00222895.1983.10735302>.
- Yaserifar, M., Souza Oliveira, A., 2022. Surface EMG variability while running on grass, concrete and treadmill. *J. Electromyogr. Kinesiol.* 62, 102624. <https://doi.org/10.1016/j.jelekin.2021.102624>.